Glasnik hemičara i tehnologa Bosne i Hercegovine

Bulletin of the Chemists and Technologists of Bosnia and Herzegovina

2017

47

49-58

Print ISSN: 0367-4444
Online ISSN: 2232-7266

UDC: _____

Original Scientific Paper

Development and validation of the mathematical model for synthesis of maleic anhydride from *n*-butane in a fixed bed reactor

Petric, I., Karić E.*

Department of Chemical Engineering, Faculty of Technology, University of Tuzla, Univerzitetska 8, 75000 Tuzla, Bosnia and Herzegovina

Article info
Received:14/10/2016
Accepted: 28/12/2016

Keywords:
modeling
n-butane
maleic anhydride
fixed bed reactor
simulation
kinetic models

Corresponding author: Ervin Karić
E-mail: ervin.karic@untz.ba
Phone: +387 60 321-5468
Fax: +387 35 320-741

Abstract: The aims of this study were the following: development of the mathematical model for numerical simulation of partial oxidation of *n*-butane to maleic anhydride in a fixed bed reactor and validation of developed mathematical model with real process data from industrial reactor located in the Global Ispat Coke Industry Lukavac. Mathematical model is consisted of differential equations that describe mass balances of each species, energy balance, stoichiometry of reactions, pressure drop, kinetic model. Numerical software package Polymath with Runge-Kutta-Fehlberg method was used for numerical solution of differential equations. The developed mathematical model was validated with three process data sets of five measured variables (temperature, pressure, concentration of *n*-butane, concentration of carbon dioxide, concentration of carbon monoxide) and with application of ten kinetic models from literature. Comparison of simulation results and measured data showed a good agreement for three kinetic models. For the chosen kinetic model, profiles of temperature, molar flows, conversion of *n*-butane and selectivity of maleic anhydride were also presented.

INTRODUCTION

Maleic anhydride is a chemical compound with multiple applications in the chemical industry. It is used for the production of polyester and alkyd resins, additives for lubricating oil, as the acid in the food industry, polymeric materials etc. When *n*-butane replaced benzene as a raw material for the production of maleic anhydride, it has enabled the development of highly active and selective catalyst. New process for the production of maleic anhydride enabled higher yields with lower investments. Higher yields of maleic anhydride are achieved with oxygen concentration lower than its stoichiometric amount. Among many industrial processes, partial oxidation of *n*-butane to maleic anhydride has received a special attention because of its economic profitability as well as a high demand for maleic anhydride as chemical product. Modern commercial processes for the production of the maleic anhydride are based on a selective oxidation of *n*-butane over a vanadium-phosphorus oxide catalyst in fixed bed reactors and fluidized bed reactors (Dente *et al*., 2003). Fixed bed reactor is well known technology, whose improvement is based on the modification of catalyst rather than design of a reactor. Cruz-Lopez *et al*. (2005) investigated the selective oxidation of *n*-butane in a membrane reactor. They used a high concentration of *n*-butane. Fixed bed reactor is limited to processes with a low concentration of *n*-butane (below 2%), while a fluid bed reactor can operate with a higher concentration of *n*-butane. Gascón *et al*. (2006) investigated the kinetics of oxidation of *n*-butane to maleic anhydride over a vanadium catalyst of commercial phosphorus under aerobic and anaerobic conditions in the temperature range from 400 to 435ºC. Fluid bed reactor has higher efficiency for heat removal, better temperature control and a lower yield of maleic anhydride compared to fixed bed reactor. Diedenhoven *et al*. (2012) developed a model for dynamics of phosphoric oxidation of *n*-butane to

maleic anhydride with a vanadium-phosphorus-oxide catalyst. The model showed that reverse sorption processes determine the content of phosphorus in the catalyst which is based on a vanadium-phosphorus oxide. With addition of certain phosphorus concentration, the loss can be compensated, while exceed of phosphorus concentration can cause a complete deactivation of the catalyst. Trifirò and Graseli (2014) analyzed the key aspects for oxidation of *n*-butane to maleic anhydride using a mixture of a vanadium-phosphorus oxide catalyst, in order to determine relevant parameters required for optimization of the catalyst.

Mathematical models provide a powerful tool for simulation and design of process equipment in chemical/process industry, as well as for determination of the conditions of optimal performance. Results of these studies can serve as useful guidelines for improving the design and operation of the plants well as for improving the performance of the whole process without a need for expensive tests on the plant.

The aims of this study were the following: development of the mathematical model for numerical simulation of partial oxidation of *n*-butane to maleic anhydride in a fixed bed reactor and validation of developed mathematical model with real process data from industrial reactor located in the Global Ispat Coke Industry Lukavac.

MATHEMATICAL MODEL

The following assumptions and simplifications were taken into account while developing the model:

- there are no radial gradients of temperature and concentration in the reactor,
- a reactor operates in a steady-state,
- pseudo one-dimensional model is used,
- pressure drop coefficient is assumed,
- overall heat transfer coefficient is taken from the reference Sharma *et al*. (1991).

The mechanism of reaction set I (in the case of application of the kinetics models (12) and (13)).

The main reaction:

$$n-C_4H_{10}+3.5O_2 \rightarrow C_4H_2O_3+4H_2O \quad (1)$$

Side reactions:

$$n-C_4H_{10}+6.5O_2 \rightarrow 4CO_2+5H_2O \quad (2)$$

$$C_4H_2O_3+3O_2 \rightarrow 4CO_2+H_2O \quad (3)$$

The mechanism of reaction set II (in the case of application of the kinetics models (7), (8), (9), (10), (11), (14), (15) and (16)).

The main reaction:

$$n-C_4H_{10}+3.5O_2 \rightarrow C_4H_2O_3+4H_2O \quad (4)$$

Side reactions:

$$n-C_4H_{10}+4.5O_2 \rightarrow 4CO+5H_2O \quad (5)$$

$$n-C_4H_{10}+6.5O_2 \rightarrow 4CO_2+5H_2O \quad (6)$$

The investigated kinetic models are:

Alonso *et al*. (2001):

$$r_1=\left\{1.96\cdot e^{\left[-\frac{125000}{R}\cdot\left(\frac{1}{T}-\frac{1}{653}\right)\right]}\right\}\cdot\frac{C_B}{\left[1+\frac{59\cdot C_B}{C_O}+\frac{26\cdot C_M}{C_O}\right]}$$

$$r_2=\left\{0.86\cdot e^{\left[-\frac{145000}{R}\left(\frac{1}{T}-\frac{1}{653}\right)\right]}\right\}\cdot\frac{C_B}{\left[1+\frac{59\cdot C_B}{C_O}+\frac{26\cdot C_M}{C_O}\right]}$$

$$r_3=\left\{0.07\cdot e^{\left[-\frac{180000}{R}\left(\frac{1}{T}-\frac{1}{653}\right)\right]}\right\}\cdot\frac{C_M}{\left[1+\frac{59\cdot C_B}{C_O}+\frac{26\cdot C_M}{C_O}\right]} \quad (7)$$

$$r_1=\left\{0.61\cdot e^{\left[-\frac{116000}{R}\left(\frac{1}{T}-\frac{1}{653}\right)\right]}\right\}\cdot\frac{C_B}{\left[1+\frac{20\cdot C_B}{C_O}+\frac{12\cdot C_M}{C_O}\right]}$$

$$r_2=\left\{0.3\cdot e^{\left[-\frac{130000}{R}\left(\frac{1}{T}-\frac{1}{653}\right)\right]}\right\}\cdot\frac{C_B}{\left[1+\frac{20\cdot C_B}{C_O}+\frac{12\cdot C_M}{C_O}\right]}$$

$$r_3=\left\{0.04\cdot e^{\left[-\frac{138000}{R}\left(\frac{1}{T}-\frac{1}{653}\right)\right]}\right\}\cdot\frac{C_M}{\left[1+\frac{20\cdot C_B}{C_O}+\frac{12\cdot C_M}{C_O}\right]} \quad (8)$$

$$r_1=\left\{0.86\cdot e^{\left[-\frac{80000}{R}\left(\frac{1}{T}-\frac{1}{653}\right)\right]}\right\}\cdot\frac{C_B}{\left[1+\frac{20\cdot C_B}{C_O}+\frac{12\cdot C_M}{C_O}\right]}$$

$$r_2=\left\{0.11\cdot e^{\left[-\frac{80000}{R}\left(\frac{1}{T}-\frac{1}{653}\right)\right]}\right\}\cdot\frac{C_B}{\left[1+\frac{20\cdot C_B}{C_O}+\frac{12\cdot C_M}{C_O}\right]}$$

$$r_3=\left\{0.19\cdot e^{\left[-\frac{98000}{R}\left(\frac{1}{T}-\frac{1}{653}\right)\right]}\right\}\cdot\frac{C_M}{\left[1+\frac{20\cdot C_B}{C_O}+\frac{12\cdot C_M}{C_O}\right]} \quad (9)$$

$$\left[\frac{kmol}{kgcat\cdot s}\right]$$

Buchanan and Sundaresan (1986):

$$r_1=\left[1.96\cdot 10^{10}\cdot e^{-\frac{125000}{R\cdot T}}\right]\cdot\frac{C_B}{\left[1+\frac{59\cdot C_B}{C_O}+\frac{26\cdot C_M}{C_O}\right]}$$

$$r_2=\left[3.40\cdot 10^{11}\cdot e^{-\frac{145000}{R\cdot T}}\right]\cdot\frac{C_B}{\left[1+\frac{59\cdot C_B}{C_O}+\frac{26\cdot C_M}{C_O}\right]}$$

$$r_3=\left[1.70\cdot 10^{13}\cdot e^{-\frac{180000}{R\cdot T}}\right]\cdot\frac{C_M}{\left[1+\frac{59\cdot C_B}{C_O}+\frac{26\cdot C_M}{C_O}\right]} \quad (10)$$

$$r_1 = \left[1.16 \cdot 10^9 \cdot e^{-\frac{116000}{R \cdot T}}\right] \cdot \frac{C_B}{\left[1 + \frac{20 \cdot C_B}{C_O} + \frac{12 \cdot C_M}{C_O}\right]}$$

$$r_2 = \left[7.50 \cdot 10^9 \cdot e^{-\frac{130000}{R \cdot T}}\right] \cdot \frac{C_B}{\left[1 + \frac{20 \cdot C_B}{C_O} + \frac{12 \cdot C_M}{C_O}\right]}$$

$$r_3 = \left[4.80 \cdot 10^9 \cdot e^{-\frac{138000}{R \cdot T}}\right] \cdot \frac{C_M}{\left[1 + \frac{20 \cdot C_B}{C_O} + \frac{12 \cdot C_M}{C_O}\right]} \quad (11)$$

$$\left[\frac{kmol}{kgcat \cdot s}\right]$$

Centi *et al*. (1985):

$$r_1 = \frac{2.191 \cdot 10^{-4} \cdot 2616 \cdot C_B \cdot C_O^{0.2298}}{1 + 2616 \cdot C_B}$$

$$r_2 = 7.028 \cdot 10^{-5} \cdot C_O^{0.2298}$$

$$r_3 = 4.989 \cdot 10^{-6} \cdot C_M \cdot \left(\frac{C_O^{0.6345}}{C_B^{1.151}}\right) \quad (12)$$

$$\left[\frac{mol}{kgcat \cdot s}\right]$$

Marín *et al*. (2010):

$$r_1 = \left\{3.73 \cdot 10^{-4} \cdot e^{\left[-\frac{86515.5}{R}\left(\frac{1}{T} - \frac{1}{613}\right)\right]}\right\} \cdot \frac{C_B}{\left[1 + \frac{0.08 \cdot C_B}{C_O} + \frac{124.24 \cdot C_M}{C_O}\right]}$$

$$r_2 = \left\{8.76 \cdot 10^{-5} \cdot e^{\left[-\frac{103293.1}{R}\left(\frac{1}{T} - \frac{1}{613}\right)\right]}\right\} \cdot \frac{C_B}{\left[1 + \frac{0.08 \cdot C_B}{C_O} + \frac{124.24 \cdot C_M}{C_O}\right]}$$

$$r_3 = \left\{1.65 \cdot 10^{-4} \cdot e^{\left[-\frac{146052}{R}\left(\frac{1}{T} - \frac{1}{613}\right)\right]}\right\} \cdot \frac{C_M}{\left[1 + \frac{0.08 \cdot C_B}{C_O} + \frac{124.24 \cdot C_M}{C_O}\right]} \quad (13)$$

$$\left[\frac{mol}{kgcat \cdot s}\right]$$

Lorences *et al*. (2003):

$$r_1 = \left\{2.17 \cdot e^{\left[-\frac{54418}{R}\left(\frac{1}{T} - \frac{1}{653}\right)\right]}\right\} \cdot \frac{C_B}{\left[1 + \frac{14 \cdot C_B}{C_O} + \frac{208 \cdot C_M}{C_O}\right]}$$

$$r_2 = \left\{1.34 \cdot e^{\left[-\frac{104650}{R}\left(\frac{1}{T} - \frac{1}{653}\right)\right]}\right\} \cdot \frac{C_B}{\left[1 + \frac{14 \cdot C_B}{C_O} + \frac{208 \cdot C_M}{C_O}\right]}$$

$$r_3 = \left\{0.19 \cdot e^{\left[-\frac{66976}{R}\left(\frac{1}{T} - \frac{1}{653}\right)\right]}\right\} \cdot \frac{C_M}{\left[1 + \frac{14 \cdot C_B}{C_O} + \frac{208 \cdot C_M}{C_O}\right]} \quad (14)$$

$$\left[\frac{kmol}{kgcat \cdot s}\right]$$

Schneider *et al*. (1987):

$$r_1 = 9.66 \cdot 10^{-5} \cdot \frac{0.11 \cdot 10^{-5} \cdot p_O^{\frac{1}{2}}}{1 + 0.11 \cdot 10^{-5} \cdot p_O^{\frac{1}{2}}} \cdot p_B$$

$$r_2 = 1.72 \cdot 10^{-5} \cdot \frac{4.2 \cdot 10^{-5} \cdot p_O}{1 + 4.2 \cdot 10^{-5} \cdot p_O} \cdot p_B$$

$$r_3 = 2.21 \cdot 10^{-5} \cdot \frac{4.2 \cdot 10^{-5} \cdot p_O}{1 + 4.2 \cdot 10^{-5} \cdot p_O} \cdot p_B \quad atm \quad (15)$$

Sharma *et al*. (1991):

$$r_1 = \left\{0.96 \cdot 10^{-6} \cdot e^{\left[-\frac{93100}{R}\left(\frac{1}{T} - \frac{1}{673}\right)\right]}\right\} \cdot p_B^{0.54} \cdot (1 + 310 \cdot p_M)$$

$$r_2 = \left\{0.15 \cdot 10^{-6} \cdot e^{\left[-\frac{93100}{R}\left(\frac{1}{T} - \frac{1}{673}\right)\right]}\right\} \cdot p_B^{0.54}$$

$$r_3 = \left\{0.29 \cdot 10^{-5} \cdot e^{\left[-\frac{155000}{R}\left(\frac{1}{T} - \frac{1}{673}\right)\right]}\right\} \cdot p_M \cdot (1 + 310 \cdot p_M)^2 \quad atm \quad (16)$$

A – *n*-C_4H_{10}, B – O_2, C – $C_4H_2O_3$, D – CO_2, E – H_2O, F – CO

The molar balance of components is given by the equation:

$$\frac{dF_i}{dW} = r_i \quad (17)$$

where: i – component, F_i – molar flow of component i (kmol/h), r_i' – reaction rate for component i (kmol/(kg·h), W – mass of catalyst (kg).

The heat balance is given by the equation:

$$\frac{dT}{dW} = \frac{U \cdot a \cdot (T_a - T) + \sum_{j=1}^{m} (r_{ji} \cdot \Delta H_{Rji})}{\sum_{i=1}^{n} F_i \cdot C_{pi}} \quad (18)$$

where: i – component, j – reaction, U – overall heat transfer coefficient (kJ/(m^2·h·K)), a – area of heat exchange A per unit volume of reactor V (1/m), A – surface of heat exchange (m^2), V – volume of reactor (m^3), C_{pi} – specific heat capacity of component i (kJ/(kmol·K)), T_a – ambient temperature (K), T – temperature of the reaction mixture in reactor (K), r_{ji}' – rate of the j reaction for the i component (kmol/(kg·h)), ΔH_{Rji} – heat of the j reaction for the i component (kJ/kmol).

Concentrations of components C_i in the reactions are given by the equation:

$$C_i = C_{T0} \cdot \left(\frac{F_i}{F_T}\right) \cdot \left(\frac{T_0}{T}\right) \cdot \left(\frac{P}{P_0}\right) \quad (19)$$

where: i – number of component, C_{T0} – total concentration of reaction mixture (kmol/m^3), F_T – total molar flow of reaction mixture (kmol/h), F_i – molar flow

of component *i* (kmol/h), T_0 – inlet temperature of the reaction mixture (K), T – temperature of the reaction mixture in reactor (K), P_0 – inlet pressure of the reaction mixture (bar), P – pressure of the reaction mixture in reactor (bar).

The total inlet concentration of reaction mixture C_{T0}:

$$C_{T0} = \frac{P_0}{R \cdot T_0} \tag{20}$$

where: R – universal gas constant, (J/(mol·K)).

The total molar flow of reaction mixture F_T:

$$F_T = \sum_{i=1}^{n} F_i \tag{21}$$

Relative rates of reaction in reaction j in compact notation:

$$\frac{r_{ji}}{\upsilon_{ji}} = \frac{r_{jk}}{\upsilon_{jk}} \tag{22}$$

where: j – reaction; i,k – component, υ – stoichiometric coefficient, r – reaction rate.

The pressure drop is given by the equation:

$$\frac{dP}{dW} = -\frac{\alpha}{2} \cdot \frac{T}{T_0} \cdot \frac{P_0}{\left(\frac{P}{P_0}\right)} \cdot \frac{F_T}{F_{T0}} \tag{23}$$

where: α – pressure drop parameter (1/kg).

The conversion of *n*-butane is given by the equation:

$$X_A = \frac{F_{A0} - F_A}{F_{A0}} \tag{24}$$

where: F_{A0} – inlet molar flow of *n*-butane (kmol/h), F_A – outlet molar flow of *n*-butane (kmol/h).

The yield of maleic anhydride is given by the equation:

$$\tilde{Y}_C = \frac{F_C}{F_{A0} - F_A} \tag{25}$$

where: F_C – outlet molar flow of maleic anhydride (kmol/h).

The selectivity of maleic anhydride is given by the equation:

$$\tilde{S}_{CE} = \frac{F_C}{F_E} \tag{26}$$

where: F_E – outlet molar flow of water (kmol/h).

Input data for mathematical model are: T_0=431.15 K, P_0=134000 Pa, F_{A0}=20.98 kmol/h, F_{B0}=262.1 kmol/h, F_{D0}=0.4 kmol/h, F_{E0}=6.72 kmol/h, T_a=683.15 K, W=0.6359 kg, U=107 W/(m^2·K), α=0.8 kg^{-1}, A=0.00035 m^2, V=0.0013 m^3, a=0.26923 m^{-1}, R=8.314 J/(mol·K).

$$\Delta\hat{H}_R^{(I)} = -1242655.575 + 8.039 \cdot T + 0.0124025 \cdot T^2 - 0.00004 \cdot T^3 + 1.85255 \cdot 10^{-8} \cdot T^4 \text{ (J/mol)} \tag{27}$$

$$\Delta\hat{H}_R^{(II)} = -2646628.37 + 48.939 \cdot T + 0.013971 \cdot T^2 - 0.0000517 \cdot T^3 + 3.07003 \cdot 10^{-8} \cdot T^4 \text{ (J/mol)} \tag{28}$$

$$\Delta\hat{H}_R^{(III)} = -1428408 + 40.9 \cdot T - 0.026385 \cdot T^2 - 0.0000119333 \cdot T^3 + 1.2141 \cdot 10^{-8} \cdot T^4 \text{ (J/mol)} \tag{29}$$

$$C_{PA} = 9.487 + 0.3313 \cdot T - 1.108 \cdot 10^{-4} \cdot T^2 - 2.2821 \cdot 10^{-9} \cdot T^3 \text{ (J/(mol·K))} \tag{30}$$

$$C_{PB} = 28.106 - 3.68 \cdot 10^{-6} \cdot T + 1.475 \cdot 10^{-5} \cdot T^2 - 1.065 \cdot 10^{-8} \cdot T^3 \text{ (J/(mol·K))} \tag{31}$$

$$C_{PC} = -13.075 + 0.3484 \cdot T - 2.184 \cdot 10^{-4} \cdot T^2 + 4.839 \cdot 10^{-8} \cdot T^3 \text{ (J/(mol·K))} \tag{32}$$

$$C_{PD} = 19.975 + 7.343 \cdot 10^{-2} \cdot T - 5.601 \cdot 10^{-5} \cdot T^2 + 1.715 \cdot 10^{-8} \cdot T^3 \text{ (J/(mol·K))} \tag{33}$$

$$C_{PE} = 32.243 + 1.923 \cdot 10^{-3} \cdot T + 1.055 \cdot 10^{-5} \cdot T^2 - 3.596 \cdot 10^{-9} \cdot T^3 \text{ (J/(mol·K))} \tag{34}$$

$$C_{PF} = 30.896 - 1.285 \cdot 10^{-2} \cdot T + 2.789 \cdot 10^{-5} \cdot T^2 - 1.271 \cdot 10^{-8} \cdot T^3 \text{ (J/(mol·K))} \tag{35}$$

Numerical software package Polymath with Runge-Kutta-Fehlberg method was used for a numerical solution of differential equations.

RESULTS AND DISCUSSION

Tables 1-3 show comparisons of the results of numerical simulations with measured values of outlet process parameters, differences between numerical simulations results and measured values of outlet process parameters, and percentage deviations of the numerical simulations results from measured values of outlet reactor process parameters. From October 2015, the reactor in the Global Ispat Coke Industry Lukavac operates with a new catalyst Polycat MAC 4 ML (manufacturer POLYNT, Italy). The measured outlet process parameters are: temperature, pressure, volume percentages of *n*-butane, carbon dioxide and carbon monoxide. The best agreement of simulation results and measured values was achieved with application of the kinetic model (15) by Schneider *et al.* (1987) for December 2015 and February 2016, while the best agreement for January 2016 was achieved with application of the kinetic model (16) by Sharma *et al.* (1991).

Table 1: Comparisons of results of numerical simulation and measured values of outlet process parameters.

Kinetic model		T_{out} (K)	P_{out} (bar)	% *n-butane*	% CO_2	% *CO*
Measured value	A	682.74	0.664	0.29	1.05	1.03
	B	678.9	0.672	0.28	1.08	1.06
	C	683.15	0.662	0.30	1.30	1.06
(7)		650.12	0.644	0.48	3.43	4.58
(8)		657.04	0.622	0.40	3.08	2.01
(9)		640.69	0.659	0.47	2.72	5.42
(10)		650.32	0.644	0.49	3.43	142
(11)		651.97	0.643	0.37	2.89	2.89
(12)		674.09	0.610	0.86	0.91	-
(13)		673.03	0.615	0.43	2.19	-
(14)		628.99	0.689	0.55	4.26	2.12
(15)		682.75	0.601	0.79	0.84	1.21
(16)		678.51	0.603	0.82	0.87	1.05

Legend: A - average values for December 2015, B - average values for January 2016, C - average values for February 2016, T_{out} – outlet temperature of the reaction mixture (K), P_{out} – outlet pressure of the reaction mixture (bar), %butane - oulet volume percentage of *n*-butane, %CO_2 - outlet volume percentage of carbon dioxide, %CO - outlet volume percentage of carbon monoxide.

Table 2: Differences between results of numerical simulation and measured values of outlet process parameters.

Kinetic model	T_{out} (%)	P_{out} (%)	% *n-butane (%)*	% CO_2(%)	% *CO (%)*
	4.78	3.01	-65.52	-226.67	-344.66
(7)	4.24	4.17	-71.43	-217.59	-332.08
	4.84	2.72	-60.00	-163.85	-332.08
	3.76	6.33	-37.93	-193.33	-95.15
(8)	3.22	7.44	-42.86	-185.19	-89.62
	3.82	6.04	-33.33	-136.92	-89.62
	6.16	0.75	-62.07	-159.05	-426.21
(9)	5.67	1.93	-67.86	-151.85	-411.32
	6.21	0.45	-56.67	-109.23	-411.32
	4.75	3.01	-68.97	-226.67	-37.86
(10)	4.21	4.17	-75.00	-217.59	-33.96
	4.8	2.72	-63.33	-163.85	-33.96
	4.51	3.16	-27.59	-175.24	-180.58
(11)	3.97	4.32	-32.14	-167.59	-172.64
	4.56	2.87	-23.33	-122.31	-172.64
	1.27	8.13	-196.55	13.33	-
(12)	0.71	9.23	-207.14	15.74	-
	1.33	7.85	-186.67	30.00	-
	1.42	7.38	-48.28	-108.57	-
(13)	0.86	8.48	-53.57	-102.78	-
	1.48	7.10	-43.33	-68.46	-
	7.87	-3.77	-89.66	-305.71	-105.83
(14)	7.35	-2.53	-96.43	-294.44	-100.00
	7.93	-4.08	-83.33	-227.69	-100.00
	0.001	9.49	-172.41	20.00	-17.48
(15)	-0.57	10.57	-182.14	22.22	-14.15
	0.059	9.21	-163.33	35.38	-14.15
	0.62	9.19	-182.76	17.14	-1.94
(16)	0.057	10.27	-192.86	19.44	0.94
	0.68	8.91	-173.33	33.08	0.94

The best agreement of simulation values for outlet pressure and measured values was achieved with application of the kinetic model (9) by Alonso *et al.* (2001). The best agreement of simulation values for volume percentage of *n*-butane and measured values was achieved with application of the kinetic model (11) by Buchanan and Sundaresan (1986). The best agreement of simulation values for outlet volume percentage of carbon dioxide and measured values was achieved with application of the kinetic model (12) by Centi *et al.* (1985).

The best agreement of simulation values for outlet volume percentage of carbon monoxide and measured values was achieved with application of the kinetic model (16) by Sharma *et al.* (1991). Larger deviations of simulation values of outlet volume percentages *n*-butane, carbon dioxide and carbon monoxide, for some kinetic models, probably occurred due to the simplified reaction schemes and simplified reactor model. The largest and the least deviations for the outlet temperature of reaction mixture were observed with application of the kinetic model (14) by Lorences *et al.* (2003), and with application of the kinetic model (15) by Schneider *et al.* (1987). The largest and the least deviations for the outlet pressure of reaction mixture were observed with application of the kinetic model (15) by Schneider *et al.* (1987) and with application of the kinetic model (9) by Alonso *et al.* (2001). The largest and the least deviations for the outlet volume percent of *n*-butane were observed with application of the kinetic model (16) by Sharma *et al.* (1991) and with application of the kinetic model (11) by Buchanan and Sundaresan (1986). The largest and the least deviations for the outlet volume percent of carbon dioxide were observed with application of the kinetic model (14) by Lorences *et al.* (2003) and with application of the kinetic model (12) by Centi *et al.* (1985). The largest and the least deviations for the outlet percent of reaction mixture were observed with application of the kinetic model (9) by Alonso *et al.* (1991) and with application of the kinetic model (16) by Sharma *et al.* (1991).

Table 3: Percentage deviations of results of numerical simulation from measured values of outlet reactor process parameters.

Kinetic model	T_{out} *(K)*	P_{out} (bar)	% *n-butane*	% CO_2	% *CO*
	32.62	0.02	-0.19	-2.38	-3.55
(7)	28.78	0.028	-0.2	-2.35	-3.52
	33.03	0.018	-0.18	-2.13	-3.52
	25.7	0.042	-0.11	-2.03	-0.98
(8)	21.86	0.05	-0.12	-2.00	-0.95
	26.11	0.04	-0.1	-1.78	-0.95
	42.05	0.005	-0.18	-1.67	-4.39
(9)	38.21	0.013	-0.19	-1.64	-4.36
	42.46	0.003	-0.17	-1.42	-4.36
	32.42	0.02	-0.2	-2.38	-0.39
(10)	28.58	0.028	-0.21	-2.35	-0.36
	32.83	0.018	-0.19	-2.13	-0.36
	30.77	0.021	-0.08	-1.84	-1.86
(11)	26.93	0.029	-0.09	-1.81	-1.83
	31.18	0.019	-0.07	-1.59	-1.83
	8.65	0.054	-0.57	0.14	-
(12)	4.81	0.062	-0.58	0.17	-
	9.06	0.052	-0.56	0.39	-
	9.71	0.049	-0.14	-1.14	-
(13)	5.87	0.057	-0.15	-1.11	-
	10.12	0.047	-0.13	-0.89	-
	53.75	-0.025	-0.26	-3.21	-1.09
(14)	49.91	-0.017	-0.017	-3.18	-1.06
	54.16	-0.027	-0.027	-2.96	-1.06
	-0.01	0.063	0.063	0.21	-0.18
(15)	-3.85	0.071	0.071	0.24	-0.15
	-0.4	0.061	0.061	0.46	-0.15
	4.23	0.061	0.061	0.18	-0.02
(16)	0.39	0.069	0.069	0.21	0.01
	4.64	0.059	0.059	0.43	0.01

Figures 1-10 show a comparison of simulated and measured values for temperatures of the reaction mixture along reactor length for different kinetic models that were used in the simulation.

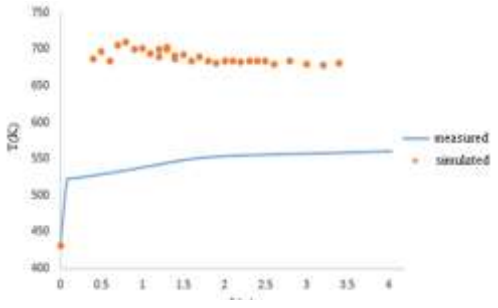

Figure 1: Comparison of simulation and measured values for temperature of reaction mixture reactor length, in the kinetic model (7) by Alonso *et al.* (2001

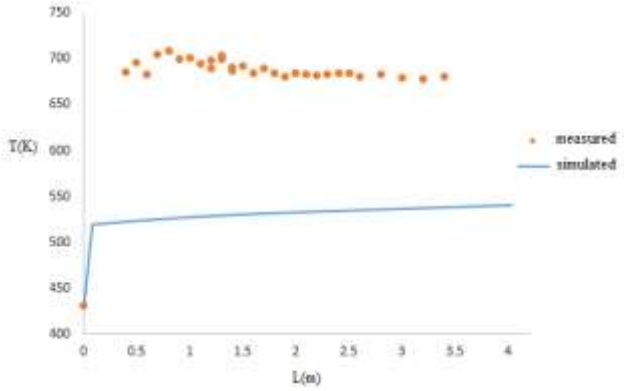

Figure 2: Comparison of simulation and measured values for temperature of reaction mixture along reactor length, in the kinetic model (8) by Alonso *et al*. (2001).

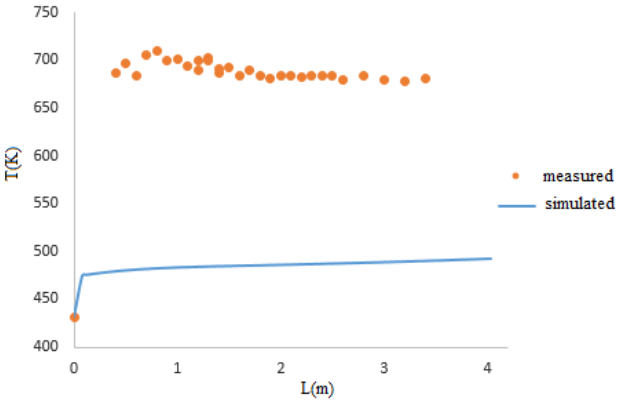

Figure 3: Comparison of simulation and measured values for temperature of reaction mixture along reactor length, in the kinetic model (9) by Alonso *et al*. (2001).

Alonso *et al*. (2001) investigated the kinetics (kinetic models (7), (8) and (9)) in a pilot membrane reactor with fluid bed of catalyst (located inside the porous membrane). The application of kinetics obtained from a fluidized bed reactor on industrial fixed bed reactor is the main reason for a poor agreement of simulation results and measured values.

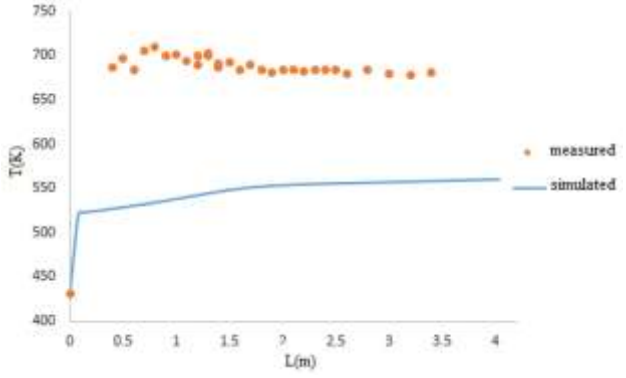

Figure 4: Comparison of simulation and measured values for temperature of reaction mixture along reactor length, in the kinetic model (10) by Buchanan and Sundaresan (2001).

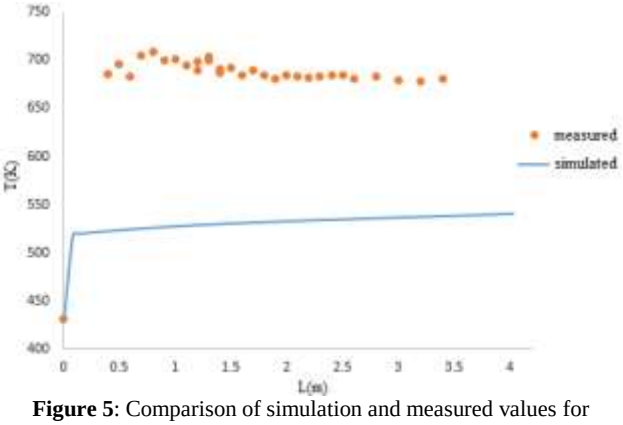

Figure 5: Comparison of simulation and measured values for temperature of reaction mixture along reactor length, in the kinetic model (11) by Buchanan and Sundaresan (2001).

Buchanan and Sundaresan (1986) investigated the kinetic models (10) and (11) and determined the kinetics for partial oxidation of *n*-butane over a vanadium phosphate catalyst. They also determine the effect of phosphorus on the kinetics of the oxidation of *n*-butane. They used a tubular reactor with internal tube diameter of 7 mm and catalyst diameter of 4 mm. These values significantly differ from the values in the industrial plant of Global Ispat Coke Industry Lukavac (internal diameter tubes 21 mm, catalyst diameter 2 mm) and this fact had a major impact on a poor agreement of simulation results and measured values in the present study.

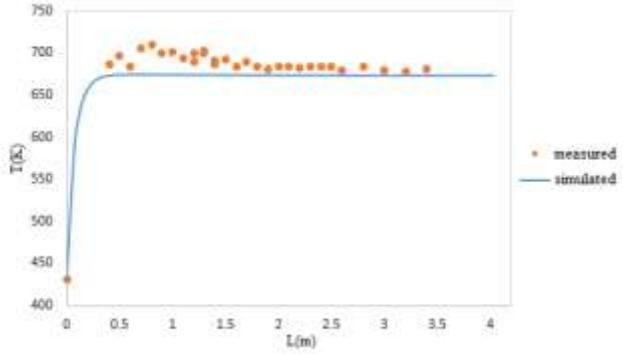

Figure 6: Comparison of simulation and measured values for temperature of reaction mixture along reactor length, in the kinetic model (12) by Centi *et al*. (1985).

Centi *et al*. (1985) investigated the kinetic model (12) and they used a fixed bed reactor based on a vanadium-phosphorus oxide. Inlet temperature was between 370 and 410°C. Simulated temperatures of the reaction mixture along reactor length with kinetic model (6) show good agreement with measured values in the present study, due to the use of similar type of reactor and the same type of catalyst. The kinetic model (14) uses the concentrations of *n*-butane, oxygen, and maleic acid.

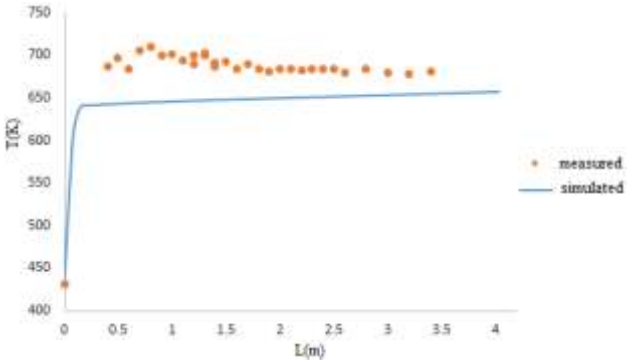

Figure 7: Comparison of simulation and measured values for temperature of reaction mixture along reactor length, in the kinetic model (13) by Marín *et al*. (2010).

Marín *et al*. (2010) investigated the kinetic model for partial oxidation of *n*-butane to maleic anhydride in a membrane reactor with enhanced heat transfer through the membrane walls. They also investigated the influence of the reactor length, flow rate of gas phase, inlet temperature of reaction mixture and inlet concentration of *n*-butane on *n*-butane conversion and selectivity of maleic anhydride. They used fixed bed reactor with the catalyst tubes (inner diameter of 34 mm, length of 0.5 m). In the industrial plant of Global Ispat Coke Industry Lukavac, a reactor tube with inner diameter 21 mm and length of 3.7 m was used. Therefore, the differences in the main dimensions of reactor (laboratory reactor versus industrial reactor) were possible cause of a poor agreement of simulation results and measured values in the present study. The kinetic model (13) uses the concentration of *n*-butane, oxygen, and maleic acid.

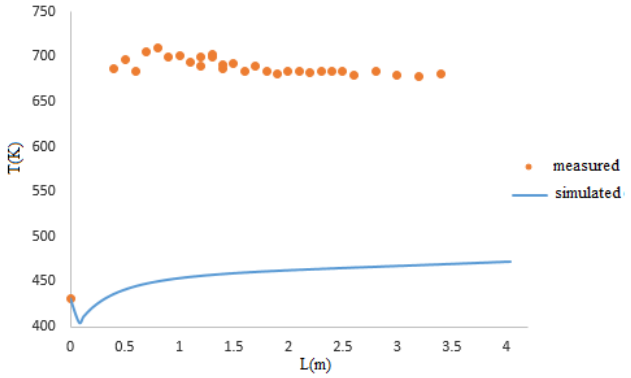

Figure 8: Comparison of simulation and measured values for temperature of reaction mixture along reactor length, in the kinetic model (14) by Lorences *et al*. (2003).

Lorences *et al*. (2003) investigated the kinetic model (14) with a wide range of operating conditions in order to assess their impacts on environmental pollution, the selectivity of maleic anhydride, bio-based products, productivity and reaction rate. The experiment was performed with a catalyst based on a vanadium-phosphorus oxide in a fluid bed reactor (inner diameter 0.04 m, height of 0.79 m). Volume percentages of *n*-butane at reactor inlet were 2, 5 and 9%. In the industrial reactor of Global Ispat Coke Industry Lukavac, volume percentage of *n*-butane at reactor inlet is 1.65%. The differences in the inlet volume percentages of *n*-butane is probably the main reason for a poor agreement of simulation and measured values in the present study. Moreover, kinetic model (14) uses the concentrations of *n*-butane, oxygen, and maleic acid.

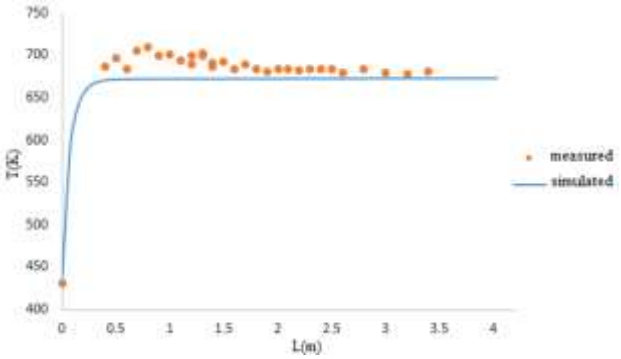

Figure 9: Comparison of simulation and measured values for temperature of reaction mixture along reactor length, in the kinetic model (15) by Schneider *et al*. (1987).

Schneider *et al*. (1987) investigated the kinetics (kinetic model (15)) of the oxidation of *n*-butane over a catalyst based on a vanadium-phosphorus oxide (reactor length of 6.5 m, internal diameter of tube 1.15 cm). Simulation values of temperatures of the reaction mixture along reactor length for the kinetic model (15) show a good agreement with measured values (Figure 9) in the present study. The kinetic model (15) uses the partial pressures of *n*-butane, oxygen, and maleic acid.

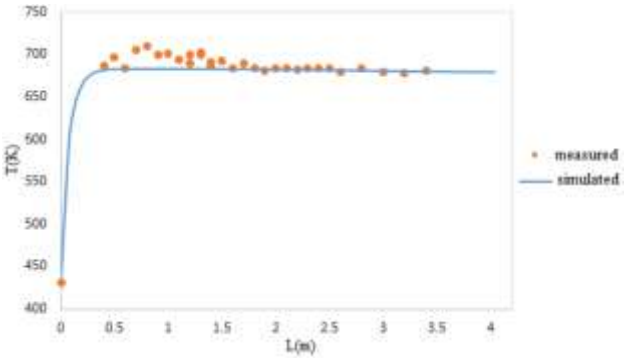

Figure 10: Comparison of simulation and measured values for temperature of reaction mixture along reactor length, in the kinetic model (16) by Sharma *et al*. (1991).

Sharma *et al*. (1991) investigated the kinetic model of selective oxidation of *n*-butane to maleic anhydride (kinetic model (16)). They used data from commercial fixed bed reactor with a catalyst based on a vanadium-phosphorus oxide. The volume percentage of butane at the reactor was 1.81%. The kinetic model used the partial pressures of *n*-butane, oxygen, and maleic acid. Simulation values of temperature of reaction mixture along reactor length show good agreement with measured values (Figure 10) in the present study. The same type of reactor and similar type of catalyst was used in industrial plant of Global Ispat Coke Industry Lukavac. Figures 11-16 show the conversion of *n*-butane, the yield of maleic anhydride, the selectivity of maleic anhydride, the molar flow rate of *n*-butane, the molar flow rate of maleic anhydride, the molar flow rate of oxygen, all along reactor length (the application of kinetic model by Sharma *et al*. (1991)).

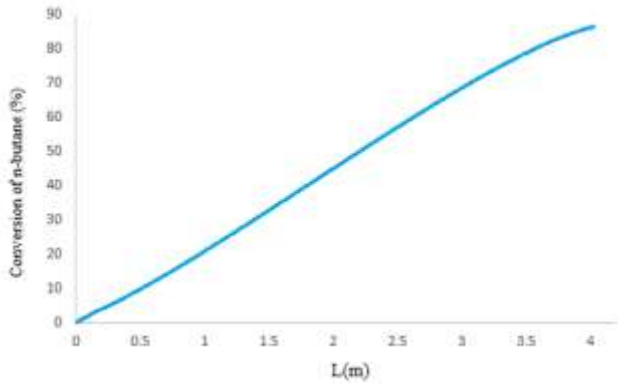

Figure 11: Conversion of *n*-butane along reactor length.

Centi *et al*. (1985) investigated the dependence of the conversion of *n*-butane as a function of space time from the physical inputs of the reaction mixture in the reactor to the exit of the reaction mixture from the reactor. Space time is correspondent with length of the reactor tube. The conversion of *n*-butane is increased by the space-time reactor, as shown in the present study.

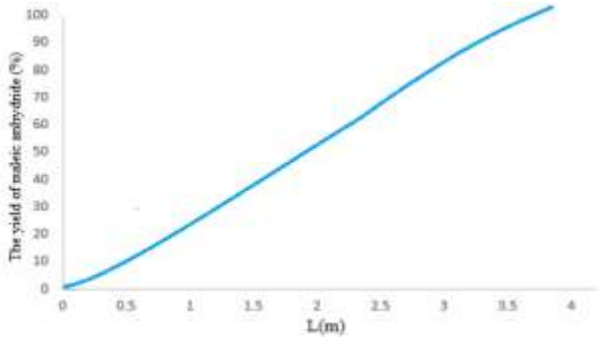

Figure 12: Yield of maleic anhydride along reactor length.

Alonso *et al*. (2001) investigated the yield of maleic anhydride by the length of the reactor tube. They found that the yield of maleic anhydride along reactor length, which has been shown in this study.

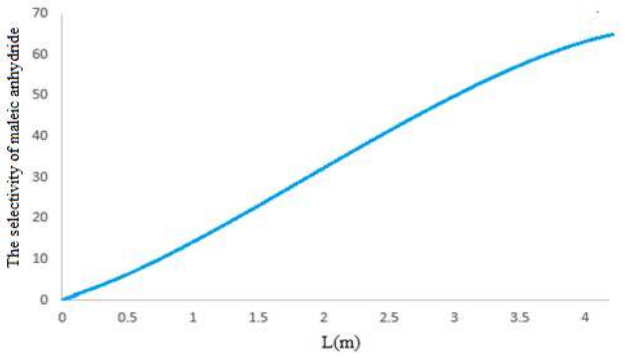

Figure 13: Selectivity of maleic anhydride along reactor length.

Moser and Schrader (1984) investigated the selectivity of maleic anhydride in a function of space time from the inlet of reaction mixture in a reactor to the outlet of reaction mixture from the reactor. The selectivity of maleic anhydride was increased with increase of space time, as it was shown in the present study.

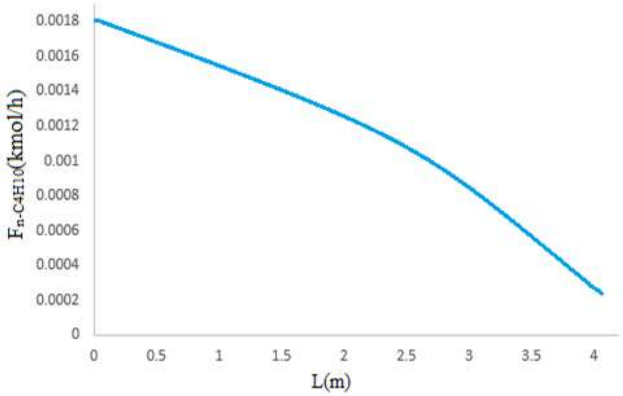

Figure 14: Molar flow rate of *n*-butane along reactor length.

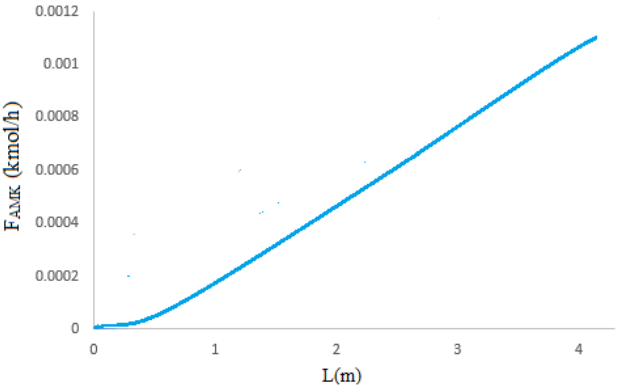

Figure 15: Molar flow rate of maleic anhydride along reactor length.

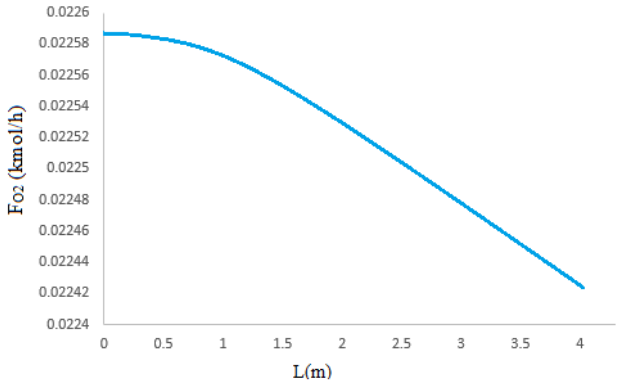

Figure 16: Molar flow rate of oxygen along reactor length.

CONCLUSIONS

The mathematical model for numerical simulation of partial oxidation of *n*-butane to maleic anhydride in a fixed bed reactor was developed. Validation of developed mathematical model was performed with real process data from industrial reactor. The mathematical model was validated with three process data sets of five measured variables (temperature, pressure, concentration of *n*-butane, concentration of carbon dioxide, concentration of carbon monoxide) and with application of ten kinetic models from literature. Comparison of simulation results and measured data showed a good agreement with application of three kinetic models: (12) (by Centi *et al*., 1985), (15) (by Schneider *et al*., 1987) and (16) (by Sharma *et al*., 1991). The profiles along reactor length for the main process parameters (conversion of *n*-butane, the yield of maleic anhydride, the selectivity of maleic

anhydride, the molar flow rate of *n*-butane, the molar flow rate of maleic anhydride, the molar flow rate of oxygen) were also analyzed. Future work is directed to improvement of the model, further validation of the model and optimization of the process performance.

REFERENCES

Alonso, M., Lorences, M.J., Pina, M.P., Patience, G.S. (2001). Butane partial oxidation in an externally fluidized bed-membrane reactor. *Catalysis Today*, *67(1-3)*, 151-157.

Buchanan, J.S., Sundaresan, S. (1986). Kinetics and Redox Properties of Vanadium Phosphate Catalysts for Butane Oxidation. *Applied Catalysis*, *26*, 211-226.

Centi, G., Fornasari, G., Trifirò, F. (1985). *n*-butane oxidation to maleic anhydride on vanadium-phospohorus oxides: Kinetic analysis with a tubular flow stacked-pellet reactor. *Industrial & Engineering Chemistry Research Development*, *24*, 32-37.

Cruz-Lopez, A., Guilhaume, N., Miachon, S., Dalmon, J.A. (2005). Selective oxidation of butane to maleic anhydride in a catalytic membrane reactor adapted to rich butane feed. *Catalysis Today*, *107-108*, 949-956.

Dente, M., Pierucci, S., Tronconi, E., Cecchini, Mr., Ghelfi, F. (2003). Selective oxidation of *n*-butane to maleic anhydride in fluid bed reactors: detailed kinetic investigation and reactor modelling. *Chemical Engineering Science*, *58*, *643-648*.

Diedenhoven, J., Reitzmann, A., Mestl, G., Turek, T. (2012). A Model for the Phosphorus Dynamics of VPO Catalysts during the Selective Oxidation of *n*-Butane to Maleic Anhydride in a Tubular Reactor. *Chemie Ingenieur Technik*, *84(4)*, 1-8.

Gascón, J., Valenciano, R., Téllez, C., Herguido, J., Menéndez, M. (2006). A generalized kinetic model for the partial oxidation of *n*-butane to maleic anhydride under aerobic and anaerobic conditions. *Chemical Engineering Science*, *61*, 6385-6394.

Lorences, M.J., Patience, G.S., Dìez, F.V., Coca, J. (2003). Butane Oxidation to Maleic Anhydride: Kinetic Modeling and Byproducts. *Industrial & Engineering Chemistry Research*, *42*, 6730-6742.

Marín, P., Hamel, C., Ordóñez, S., Dìez, F.V., Tsotsas, E., Seidel-Morgenstern, A. (2010). Analysis of a fluidized bed membrane reactor for butane partial oxidation to maleic anhydride: 2D modelling. *Chemical Engineering Science*, *65*, 3538-3548.

Moser, T.P., Schrader, G.L., 1985. Selective Oxidation of *n*-Butane to Maleic Anhydride by Model V-P-O Catalysis. *Journal of Catalysis*, *92*, 216-231.

Schneider, P., Emig, G., Hofmann, H. (1987). Kinetic investigation and reactor simulation for the catalytic gas-phase oxidation of *n*-butane to maleic anhydride. *Industrial & Engineering Chemistry Research*, *26*, 2326-2241.

Sharma, R.K., Cresswell, D.L., Newson, E.J. (1991). Kinetics and fixed-bed reactor modelling of butane oxidation to maleic anhydride. *American Institute of Chemical Engineers Journal*, *37(1)*, 39-47.

Trifirò, F., Grasselli, R. K. (2014). How the Yield of Maleic Anhydride in *n*-Butane Oxidation, Using VPO Catalysts, was Improved Over the Years. *Topics in Catalysis*, *57(14-16)*, 1188-1195.

Summary/Sažetak

Ciljevi ove studije su bili: razvoj matematičkog modela za numeričku simulaciju oksidacije *n*-butana u anhidrid maleinske kiseline u industrijskom cijevnom reaktoru sa nepokretnim slojem katalizatora i verifikacija razvijenog matematičkog modela sa stvarnim procesnim veličinama sa industrijskog reaktora koji se nalazi Global Ispat Koksna Industrija d.o.o. Lukavac. Matematički model se sastoji od diferencijalnih jednačina koje opisuju materijalni bilans svake komponente, energetski bilans, stehiometriju reakcija, pad pritiska, kinetički model. Za rješavanje diferencijalnih jednačina korišten je numerički softverski paket Polymath sa Runge-Kutta-Fehlberg metodom. Razvijeni matematički model je verificiran sa tri seta procesnih podataka od pet mjerenih varijabli (temperatura, pritisak, koncentracija *n*-butana, koncentracija ugljikovog dioksida, koncentracija ugljikovog monoksida) i sa primjenom deset kinetičkih modela preuzetih iz literature. Usporedba simulacijskih rezultata i mjerenih podataka je pokazala dobro slaganje za tri kinetička modela. Za odabrani kinetički model, prikazani su profili temperature, molarnih protoka, konverzije *n*-butana i selektivnosti anhidrida maleinske kiseline.